Materials Science-Poland
Volume 42 Issue 4 · pp. 50–65 · DOI: 10.2478/msp-2024-0044

Materials Science-Poland

Microstructure morphology and aging characteristics of 9% Cr martensitic heat-resistant steel after service

Research Article

Zhang Kun[1], Cai Wenhe[2], Wang Zhichun[3], Xin Chen[1], Fengyuan Shu[4], Shi Yang[5], Jianwei Wang[5], Li Weili[2], Zhang Xin[6]*

[1] *China Nuclear Energy Technology Co., Ltd., Beijing, 100193, China*
[2] *North China Electric Power Test and Research Institute, China Datang Group General Institute of Science and Technology Co., Ltd., Beijing, 100040, China*
[3] *North China Electric Power Research Institute Co., Ltd., Beijing, 100096, China*
[4] *School of Chemical Engineering and Technology, Sun Yat-sen University, Zhuhai, 519082, China*
[5] *China Fire and Rescue Institute, Beijing, 102202, China*
[6] *Science and Technology Research Institute, State Power Investment Corporation, Beijing, 102209, China*

Received 02 April 2024; Accepted 26 October 2024

Abstract: Herein, based on the strengthening mechanism and aging mechanism of 9% Cr steel, changes in the microstructure and mechanical properties during long-term high-temperature service are analyzed. The limitations of current microstructure observation in the aging rating process and the defects of the aging evaluation system are expounded. It is proposed that the aging evaluation of 9% Cr martensitic heat-resistant steel can distinguish between the abnormal microstructure and the aging phenomenon occurring during long-term operation, and the combination of higher resolution microscopy observation such as laser confocal scanning microscopy with mechanical property tests could provide a comprehensive judgement.

Keywords: *9% Cr martensitic heat-resistant steel • Aging characteristics • Microstructure • Evaluation method*

1. Introduction

Ultracritical and ultrasupercritical units have developed rapidly and become the mainstream unit in the thermal power generation industry [1]. In China, the number of supercritical units with power ≥600 MW has exceeded 400 [2], many of which have been in service for over 100,000 h [3]. The metal components inside the units would gradually face a series of issues such as aging inspection, supervision, rating, replacement, and life assessment [4].

The 9% Cr martensitic heat-resistant steel has been widely used in components such as pipelines, headers, heating surfaces, valves, and connecting pipes of ultra-supercritical units [5]. P91 and P92 are widely used in high-temperature headers, pipelines, etc. [6]. The high-temperature superheater, high-temperature reheater [7], and nozzle seat of the heating surface almost all use T91 and T92[8]. The turbine rotor, high- and medium-pressure inner cylinder, valves, etc. are made of 9–12% Cr martensitic heat-resistant steel [9]. Therefore, it can be said that 9% Cr martensitic heat-resistant steel is a key material for supporting supercritical and ultrasupercritical power generation units [10]. In DL/T438-2016 "Technical Supervision Regulations for Metal in Thermal Power Plants," special inspection clauses are specified for heating surface pipes of 9% Cr steel that have been in operation for over 100,000 h, large pipelines and headers that have been in service for 3–4 A-level maintenance, etc. [11]. The purpose was to monitor and grasp the changes in 9% Cr martensitic heat-resistant steel components after long-term operation and to avoid accidents caused by material creep and aging. Therefore, it was necessary to master the microstructure and aging during operation of 9% Cr martensitic heat-resistant steel after service.

* *E-mail: kmzx201@163.com*

2. Experimental materials and methods

2.1 Experimental materials

We have mainly studied and analyzed the microstructure and aging characteristics of P91 and P92 materials after operating for about 50,000 h in one million ultrasupercritical units, in order to avoid accidents caused by material creep and aging. The actual compositions of the tested P91 and P92 materials are determined by inductively coupled plasma–atomic emission spectrometry analysis, and the results are presented in Table 1.

2.2 Experimental methods

2.2.1 Mechanical properties

From the tensile test, mechanical properties could be obtained, including the yield strength ($R_{P0.2}$) and tensile strength (R_m). The tensile test is performed on a UH-F50A (250 kN) test machine at room temperature and high temperature (600°C).

2.2.2 Investigation of the microstructure

Spark emission spectroscopy based on the GB/T 11170-2008 method is adopted to analyze the alloy composition of deposited metals. The specimen for metallographic observation is cut along the longitudinal direction of welding pass. After grinding and polishing, the specimen is etched by a mixed solution consisting of 5 g of $CuCl_2$, 30 ml of HCl, 25 ml of alcohol, and 30 ml of H_2O. Then, the microstructure of deposited metals is investigated by using an MEF-4M metallographic microscope and an SCIAS 6.0 image analysis system. The second phase of deposited metals and impact fracture surface are analyzed using a scanning electron microscope (HITACHI S-4300) coupled with an energy-dispersive spectrometer.

A transmission electron microscope (H-800) is utilized for the investigation of the fine structure and for the qualitative analysis of the second phase.

3. Aging mechanism and grading of heat-resistant steel

3.1 Aging rating of metals in power plants

Due to the relatively simple and limited variety of metallic materials used in early power plants, the aging rating of metallic materials is initially categorized according to material grade [12]. Although significant progress has been made in the aging rating of new heat-resistant steels in recent years, such as the release of DL/T 1422-2015 "Standard for Aging Rating of Microstructure of 18Cr-8Ni Series Austenitic Stainless Steel Boiler Tubes," there are still many aging mechanisms and ratings of new heat-resistant steels that urgently need to be supplemented and improved. Taking martensitic steel as an example, currently, only DL/T884-2004 "Technical Guidelines for Metallographic Inspection and Evaluation of Thermal Power Plants" provides a rough description of "microstructure aging evaluation of non-pearlite steel." However, due to the significant limitations in understanding martensitic heat-resistant steel during the standard writing period, the standards are revised based on development and industry needs [13].

3.2 Structure and morphology of typical 9% Cr martensitic heat-resistant steel

The structure of 9% Cr martensitic heat-resistant steel after strict implementation of the heat treatment process is uniform tempered martensite, with fine grains, carbide dispersed out of the grain or grain boundary, with significant lathing martensite morphology, and a high-density dislocation network in the lath martensite [14]. These

Materials	C	Mn	P	S	Si	Cr	Mo	V	Nb	N	Ni
P91	0.10	0.35	0.015	0.005	0.28	8.77	0.92	0.21	0.08	0.05	0.20

Materials	C	Mn	P	S	Si	Cr	Mo	V	W	Nb	N	B
P92	0.08	0.55	0.012	0.003	0.38	4.89	0.52	1.21	1.78	0.07	0.010	0.003

Table 1. Chemical composition of P91 and P92 (mass fraction, %).

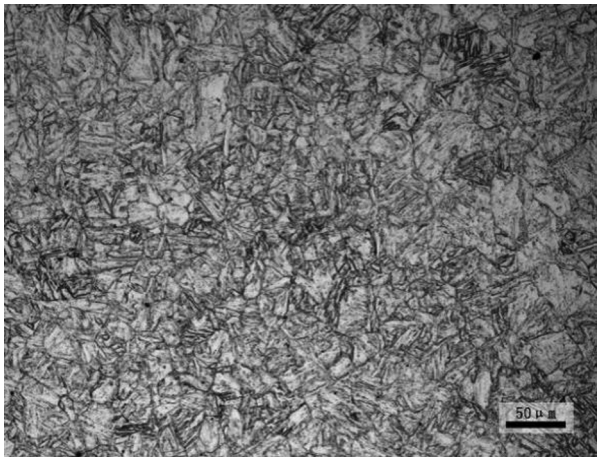

Figure 1. Metallographic morphology of P91 steel.

microstructure characteristics have a positive effect on the strengthening of martensitic steel [15]. Taking typical 9% Cr steel as an example, its metallographic structure is found to be uniform, as shown in Figure 1, the lathing martensite phase is obvious, as shown in Figure 2, the precipitation phase is fine and dispersed, and a large number of dislocations are distributed in lath martensite, as shown in Figures 3 and 4.

3.3 Strengthening mechanism of 9% Cr martensitic heat-resistant steel

Compared with traditional carbon steel and low alloy steel, 9% Cr martensitic heat-resistant steel possesses multiple strengthening factors. The main strengthening mechanism relies on the precipitation strengthening of $M_{23}C_6$, MX, and other precipitated phases, as well as the solid solution strengthening of Mo, Cr, Mn, and other elements [16].

The $M_{23}C_6$ phase is mainly composed of carbon and chromium, and the Cr-rich carbide precipitation phase is mostly nucleated and grown at the original austenite grain boundary or lathing martensite boundary, in a spherical, polygonal, or strip-like shape, with the size between 200 and 800 nm. The morphology is shown in Figures 5 and 6. $M_{23}C_6$ is the most important precipitation phase in 9% Cr martensite steel, which is the main ingredient for strengthening. It has a stability effect on the lathing martensite boundary, subgrain boundary, and original austenite grain boundary and also a certain pinning effect on the dislocation movement in martensite [17]. However, research has shown that the $M_{23}C_6$ phase grows with the increase of operating temperature and time, and the growth rate of

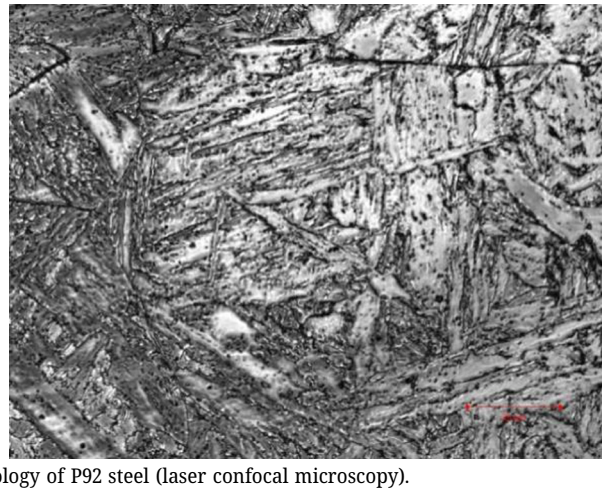

Figure 2. Metallographic morphology of P92 steel (laser confocal microscopy).

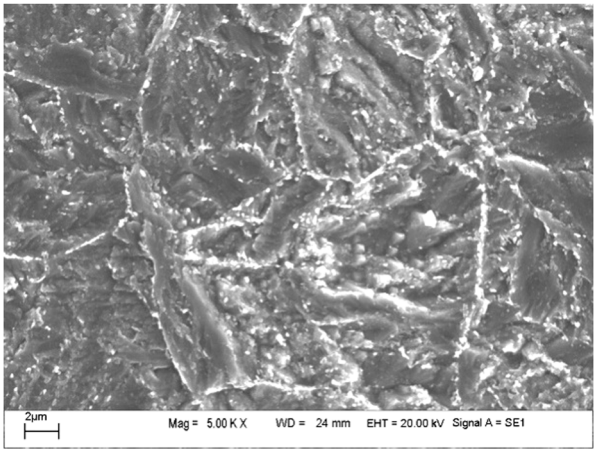

Figure 3. Microstructure morphology of P91 steel (SEM).

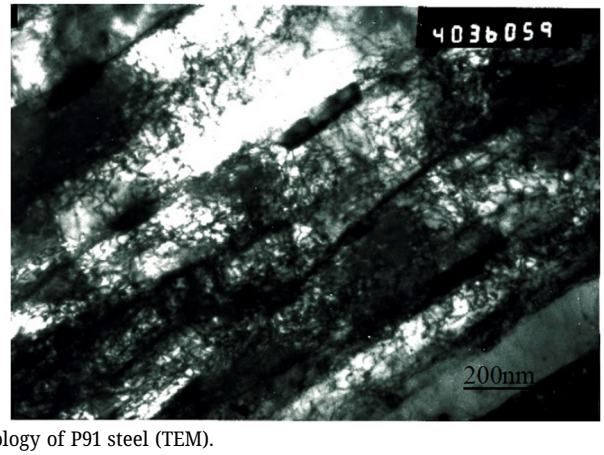

Figure 4. Microstructure morphology of P91 steel (TEM).

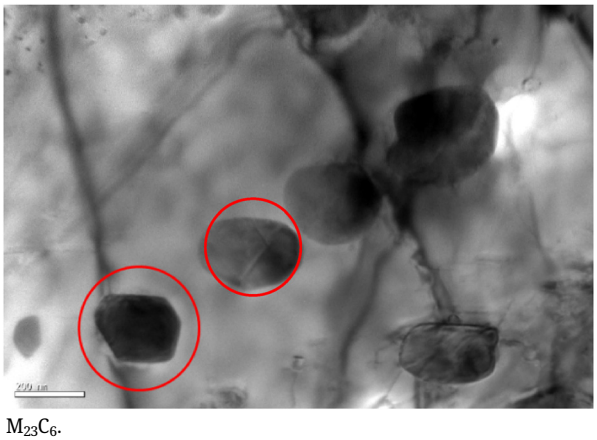

Figure 5. Polygonal and spherical $M_{23}C_6$.

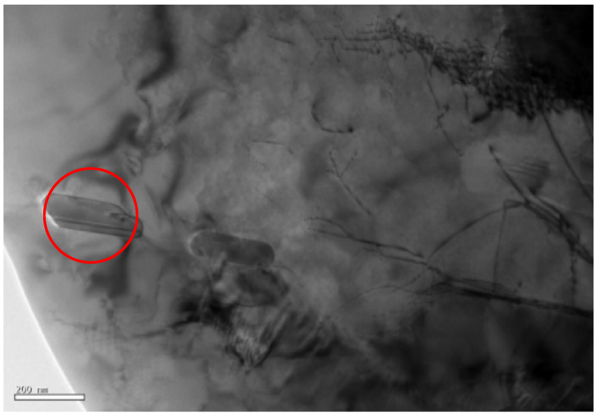

Figure 6. Strip-like $M_{23}C_6$.

$M_{23}C_6$ phase also increases with the increase of operating temperature. Therefore, after long-term high-temperature operation, the contribution of $M_{23}C_6$ to the high-temperature endurance strength of martensitic steel is weakened.

MX is a nanophase, dispersed within the crystal, with the main forms being spherical, square, rectangular, hexagonal, rod-shaped, and strip-like, as shown in Figures 7–9. Compared to $M_{23}C_6$, MX has a smaller size and higher

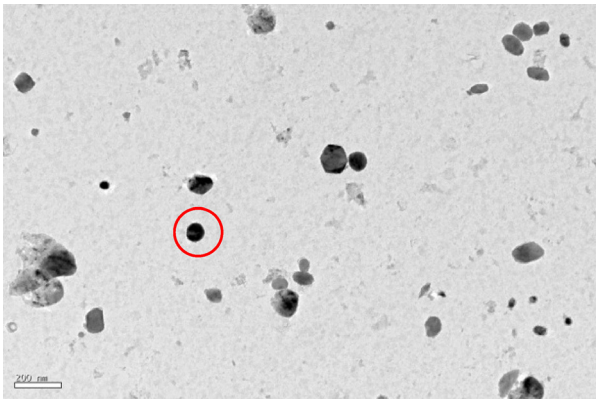

Figure 7. Spherical MX phase.

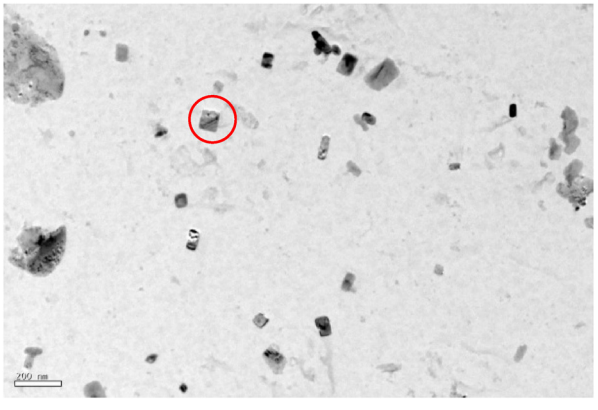

Figure 8. Cubic MX phase.

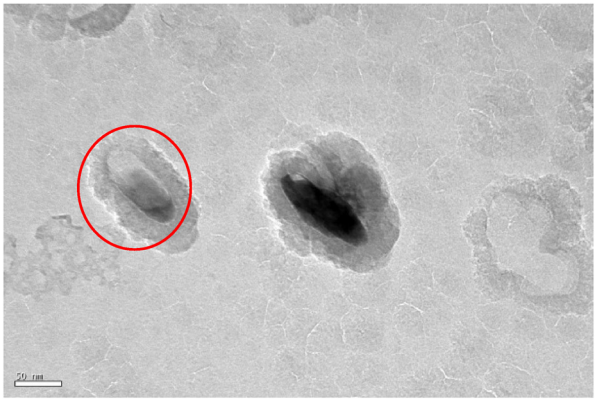

Figure 9. Short rod MX phase.

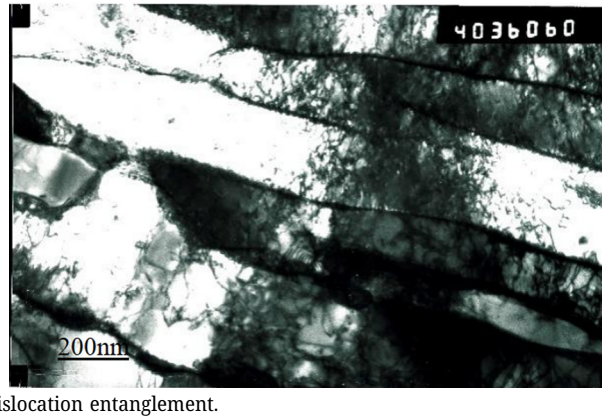

Figure 10. Martensite lath and dislocation entanglement.

stability. It is not easy to grow after long-term operation at high temperatures, and its strengthening effect would not weaken with time. MX has a significant pinning effect on dislocations in martensite, making a long-term and outstanding contribution to the stability and creep fracture strength of martensitic steel.

The lath martensite width is generally 200–400 nm, which can greatly improve the strength and toughness of the matrix and the ability to resist crack propagation. When the lath martensite is recovered at high temperatures, the lath martensite breaks up to form a smaller substructure, which could be an obstacle to dislocation

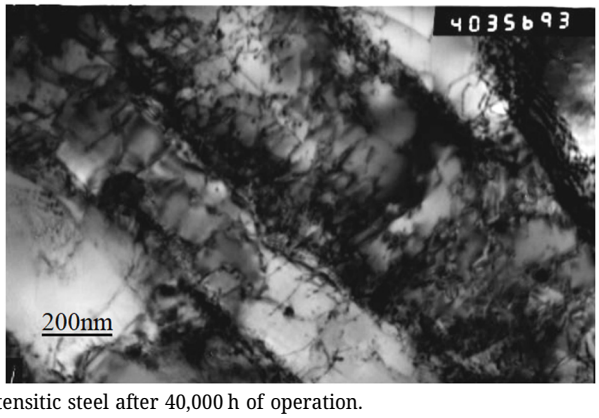

Figure 11. Microstructure of martensitic steel after 40,000 h of operation.

Figure 12. Microstructure of martensitic steel after 90,000 h of operation.

movements and facilitate achieving excellent strength of tempered lath martensite. There is a high-density dislocation network in the lath martensite, forming dislocation entanglement, which plays a significant role in strengthening the matrix, as shown in Figure 10.

Fine grains could more effectively hinder dislocation movements and improve the strength and toughness. The mechanism of multiple composite strengthening is adopted, and the improved 9% Cr martensite is added with alloying elements such as Cr, Ni, and W, all of which play a positive role in the strengthening of 9% Cr steel.

3.4 Aging mechanism of 9% Cr martensitic heat-resistant steel

Martensitic steel undergoes aging during long-term service at high temperatures, manifested by changes in the microstructure and decreased mechanical properties. The aging mechanism of martensitic steel is to some extent opposite to the strengthening mechanism. When the performance is decreased, it is inevitably accompanied by changes in the microstructure, strengthening factors, or even disappearance, such as the disappearance of martensite orientation, decrease in the dislocation density, and changes in the precipitated phase.

During the long-term high-temperature operation of martensitic steel, some dislocations disappear through slip and climb, resulting in a decrease in dislocation density. Some lath martensite boundaries disappear, and adjacent lath martensite merge into wide lath martensite or lath martensite features disappear. The phase interface of martensitic lath martensite has the effect of hindering the movement of dislocations. The widening or disappearance of lath martensite reduces the phase interface, which directly weakens the strengthening factor. The reduction or disappearance of dislocations would weaken the material's ability to resist deformation and lower its strength. Taking the microscopic morphology of pipes at different operation times and states as an example, TEM images of dislocations in lath martensite of P91 pipes after 40,000 h of operation show obvious dislocation tangles as shown in Figure 11; TEM images of dislocations in lath martensite after 90,000 h of operation at the same magnification are shown in Figure 12. It could be seen that the dislocation density was far lower than that of the microstructure of the pipeline after 40,000 h of operation. In addition, the TEM image of P91 steel bending with abnormal heat treatment under the same magnification is shown in Figure 13. It can be seen from the figure that the width of lath martensite in Figure 13 is much wider than that of lath martensite in Figure 11. The hardness of the corresponding area is about 140HB, which proves that the mechanical properties are also greatly reduced.

The transformation of the carbide structure is an important feature of aging of metallic materials. $M_{23}C_6$ and MX are the main strengthening precipitates of 9% Cr steel, of which $M_{23}C_6$ is an unstable phase. After long-term operation at high temperatures, it would grow, coarsen, and transform. Taking P92 steel as an example [18], after aging at 650°C for 26,000 h, the size of $M_{23}C_6$ is 70% larger than that before aging. Therefore, after long-term high-temperature operation, the growth of $M_{23}C_6$ phase would weaken the matrix strength, the stabilizing effect on the lathing martensite boundary and the subgrain boundary, and the effect on dislocation pinning to varying degrees, so it would weaken the contribution to the high-temperature endurance strength of martensitic steel. The MX phase is very stable and has a positive contribution to high-temperature endurance performance [19].

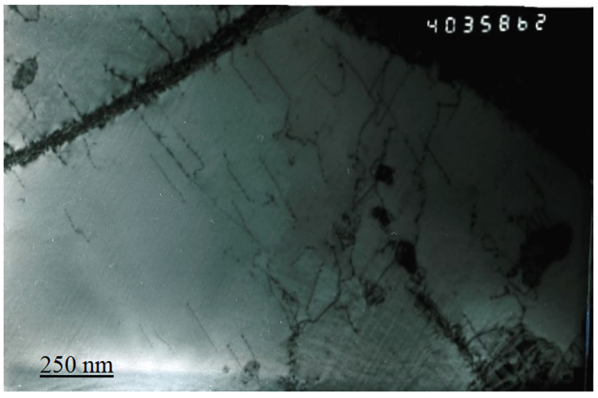

Figure 13. Microstructure of P91 steel with abnormal heat treatment.

The laves phase is a B_2A-type intermetallic compound that typically occurs under long-term service conditions above 600°C [20]. Research has shown that the laves phase would precipitate at subgrain boundaries after long-term aging, as shown in Figure 14 [21]. Although it could play a certain role in precipitation strengthening, the segregation and coarsening of the laves phase reduce its strengthening effect and consume large amounts of W and Mo, thereby reducing the solid solution strengthening effect on heat-resistant steel. Most studies suggest that after long-term aging, the Z phase would form on the basis of MX, and its precipitation leads to the consumption of the fine dispersed MX phase. In addition, the growth rate of Z phase is fast and easy to coarsen, which increase the possibility of creep pores. Therefore, the Z phase has a dual adverse effect on material creep compared to that on 9% Cr martensitic heat-resistant steel.

4. Problems encountered in organizational identification

4.1 Rating system for metal aging in power plants

At present, the aging rating of power plant metals in China is based on different material grades. However, due to the rapid development and wide variety of metals in power plants in recent decades, the existing standards are far from covering commonly used metal materials, and the aging evaluation of many materials is almost in a state of no evidence to rely on. Furthermore, there is no need to establish an evaluation standard for each material that is similar or identical (such as T91, P91, T92, P92). Therefore, the current classification of aging evaluation systems is both redundant and unreasonable. Referring to the experience

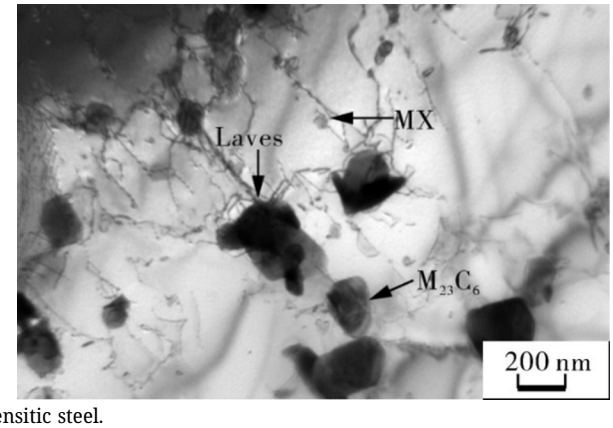

Figure 14. Laves phase in martensitic steel.

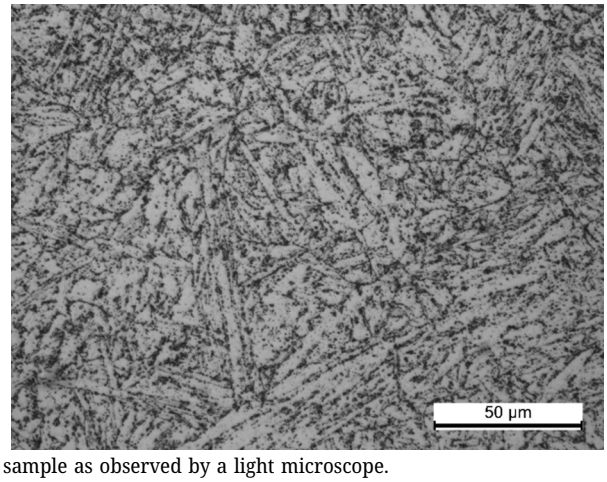

Figure 15. Microstructure of P91 sample as observed by a light microscope.

of other countries in rating the aging of metal in power plants, it is usually classified and rated according to the organizational form. From this perspective, establishing an aging rating system for common steel used in power plants is both simple and practical and more reasonable. The DL/T884 Technical Guidelines for Metallographic Inspection and Evaluation of Thermal Power Plants, which is currently being revised, is based on this point and established a classification aging rating system for pearlite steel, bainitic steel, martensitic steel, and austenitic steel.

4.2 Effect of microscopic observation on aging rating

The observation of the aging process of martensitic steel requires the use of tools to judge and analyze the changes in the microstructure, among which the most important change is the change in the precipitate phase. The main precipitate phase $M_{23}C_6$ has a size between 200 and 800 nm, and the MX size is 80–150 nm. Common metallographic examination equipment include conventional optical microscopy (OM), confocal laser scanning microscope (CLSM), scanning electron microscopy (SEM), and transmission electron microscopy (TEM).

The maximum resolution of an optical microscope is 200 nm. Due to its extremely shallow imaging depth and sample limitations, it is difficult to achieve the ideal resolution. Typically, the optimal observation magnification can be around 1,000 times, and the actual observed resolution size is about 300–600 nm. At present, the inspection and grading of the metallographic structure of 9% Cr steel is generally completed by using a conventional optical microscope. Due to its low resolution, only a relatively clear lathing martensite orientation can be seen in the observation. Carbides are faintly distributed on the matrix

Figure 16. Microstructure of P91 sample under a laser confocal microscope.

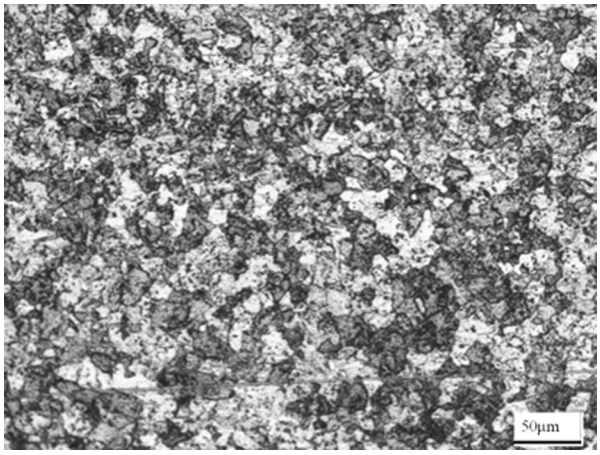

Figure 17. P92 abnormal metallographic structure of the pipeline.

and are not clear, making them difficult to identify as shown in Figure 15. From the perspective of carbide size analysis, the MX phase and most $M_{23}C_6$ phase cannot be observed, and their morphology, size, etc. cannot be distinguished. This can easily lead to deviations from the standard during the aging rating process, resulting in deviation from the rating results.

The confocal microscope uses a monochromatic laser with a shorter wavelength as the light source, with an effective resolution of up to 120 nm. It can achieve stereo-imaging and observe the distribution and morphology of the $M_{23}C_6$ phase and some MX phase, as shown in Figure 16. Therefore, LSCM, as a convenient tool with high resolution, has received widespread attention in recent years and has become a highly respected tool in practical product inspection and observation [22].

Both SEM and TEM use electron beams as the light source for microscopes, with high magnification, deep field of view, and large field of view [23]. The scale of SEM can generally reach several micrometers, while that of TEM can generally reach 20 nm. In particular, the transmission electron microscope can clearly distinguish the lathing martensite phase of the metallographic structure in the martensitic steel, the dislocation between grains, the shape and size of carbides, etc., as shown in Figures 3 and 4. However, the working environment of SEM and TEM is in a vacuum state, and they have high requirements for the sample, long observation time, and high cost, which cannot meet the requirements of on-site real-time and simple observation [24].

4.3 Common abnormal aging tissues

In the manufacturing and processing of martensitic steel, especially in the heat treatment of bent pipes and welding of pipe fittings [25], there is a process of thermal cycling. Under conditions of improper technology and poor temperature control, the structure would change, causing

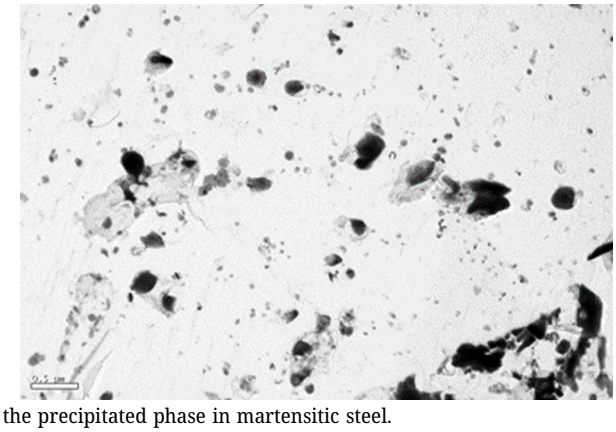

Figure 18. Abnormal growth of the precipitated phase in martensitic steel.

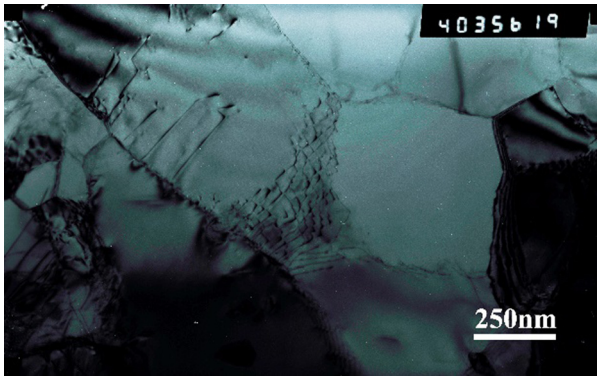

Figure 19. Ferrite appearing in martensitic steel.

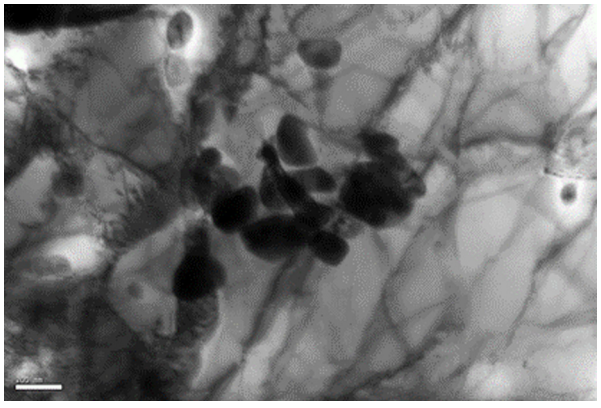

Figure 20. Disappearance of lath in martensitic steel.

abnormal aging phenomena [26]. Abnormal organization is also prone to occur in failed components such as explosive tubes. Common abnormal structures include massive ferrite, uneven grain size, disappearance of lath martensite in martensitic steel, and abnormal growth of precipitates, as shown in Figures 17–19.

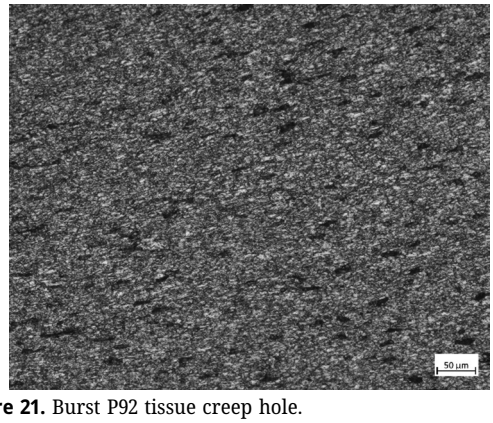

Figure 21. Burst P92 tissue creep hole.

These abnormal structures are not usually caused by long-term high temperature use, so special attention should be paid during aging rating. In some cases, they have reached the state of "severe aging" before use or at the beginning of use [27]. For example, a factory conducted metallographic inspection on P92 pipes during infrastructure construction and found that its lathing martensite morphology disappeared and polygonal block ferrite and large size precipitated phase appeared, as shown in Figures 17 and 18. Figures 19 and 20 show the microstructure morphology of the P92 pipe base metal under a transmission electron microscope, which is consistent with the observation results obtained under a light microscope. Equiaxed ferrite can be seen, and dislocation is disappeared. These phenomena indicate that serious recovery and recrystallization have occurred in this part. Tissue aging has occurred without operation.

This type of abnormal aging phenomenon is actually an accelerated aging process, which sometimes differs from the normal aging of tissues. For example, in some burst tubes, a large number of creep voids would appear

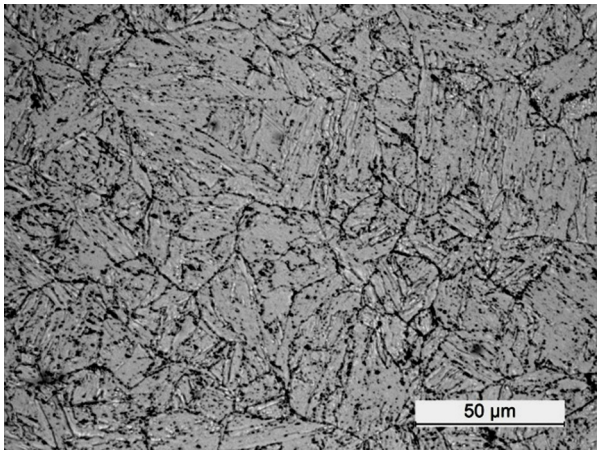

Figure 22. P91 metallographic structure after 60,000 h of operation.

as shown in Figure 21, while in actual operation aging, almost no creep voids visible under the light microscope would appear. These phenomena should be distinguished during the inspection process, and special explanations should also be provided during the rating process.

5. Aging and evaluation method of 9% Cr martensitic steel structure

5.1 Aging characteristics of 9% Cr martensitic steel

The microstructure of martensitic steel changes during long-term service at high temperatures. First, the dislocation density decreases and the width of martensitic lathing martensites increases at long-term high temperatures. Some lath martensite lose their characteristics and form massive ferrite. The reduction or disappearance of dislocations would weaken the material's ability to resist deformation. The decrease of martensitic lathing martensite phase interface would reduce the effect of hindering dislocation movements, thus aggravating the decrease of the dislocation density.

The transformation of the carbide structure is an important feature of metallic material aging. $M_{23}C_6$ and MX are the main strengthening precipitates in 9% Cr steel, among which $M_{23}C_6$ is an unstable phase. After long-term operation at high temperatures, it would undergo growth, coarsening, and transformation, which weaken the interface stability and dislocation pinning effect. The laves phase and Z phase are precipitated phases formed after long-term aging, especially the Z phase. Research has shown

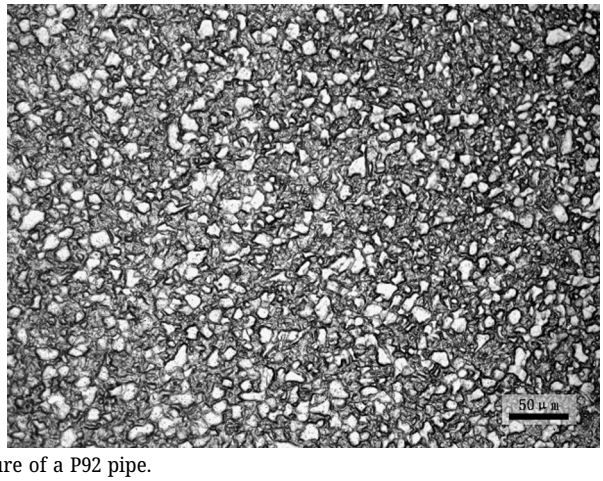

Figure 23. Metallographic structure of a P92 pipe.

Item		$R_{p0.2}$ (MPa)	R_m (MPa)	A (%)	Z (%)
Reference value (ASME SA335)		≥415	≥585	≥20	—
Actual measured value	L3-1	427	602	24.0	65
	L3-2	430	595	25.5	66

Table 2. Mechanical property test results at room temperature.

Item		$R_{p0.2}$ (MPa)	R_m (MPa)	A (%)	Z (%)
Reference value (GB5310)		≥198	—	—	—
Actual measured value	G3-1	220	305	35.0	89
	G3-2	220	310	37.0	89

Table 3. Mechanical property test results at high temperature (600°C).

that they are only discovered after at least 100,000 h of high-temperature aging above 540°C. Segregation and coarsening of the laves phase reduce the strengthening effect and consume large amounts of W and Mo, resulting in a weakened solid solution strengthening effect. The precipitation of the Z phase would consume stable and finely dispersed MX. When the Z phase grows and coarsens, it increases the possibility of creep pores. Therefore, the laves phase and the Z phase have adverse effects on the creep strength of 9% Cr martensitic heat-resistant steel.

The disappearance of martensite orientation, decrease in dislocation density, coarsening and dissolution of $M_{23}C_6$, and formation and coarsening of Z and laves phases all

Item		$R_{p0.2}$ (MPa)	R_m (MPa)
Reference value (GB5310)		415	585
Actual measured value	1#	283	560

Table 4. Mechanical property test results at room temperature.

Item		Temperature (°C)	$\sigma^{°tC}_{1\times10^5}$ (MPa)
Reference value (GB5310)		540	166
Actual measured value	2#	540	95

Table 5. High-temperature endurance test results.

contribute to a significant decrease in material creep strength, which was a typical characteristic of martensitic steel aging.

5.2 Correspondence between the metallographic structure and mechanical properties

To some extent, the microstructure of metallic materials corresponds to their mechanical properties, and aging of the microstructure would inevitably cause changes in mechanical properties.

The metallographic structure of P91 main steam pipe after about 60,000 h of operation is shown in Figure 22. Although its structure is still uniform tempered martensite, its lathing martensite orientation has been dispersed, and the orientation of some areas is not clear. Part of the precipitated phases aggregate and grow on the boundary,

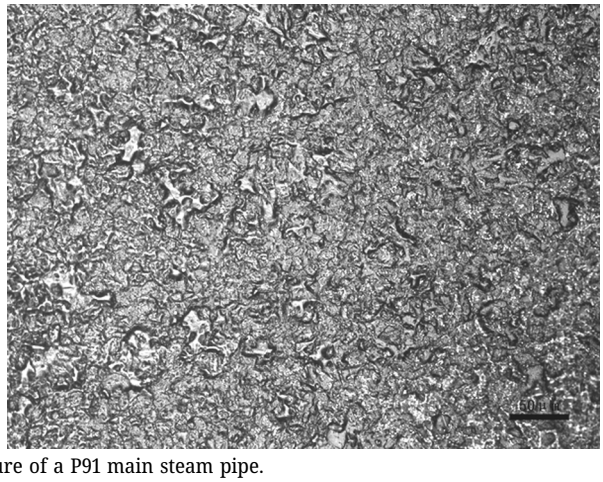

Figure 24. Metallographic structure of a P91 main steam pipe.

and their corresponding mechanical properties are shown in Tables 2 and 3. Although their mechanical properties at room temperature and high temperature meet the requirements of relevant standards, they are all within the numerical range close to the lower limit. This indicates that the metallographic structure of P91 pipeline undergoes aging during long-term high-temperature operation, accompanied by a decrease in mechanical properties.

In the early infrastructure construction process, due to limitations in understanding and processing the level of 9% Cr martensitic heat-resistant steel, there are a large number of unoperated components with abnormal structures, and the mechanical properties corresponding to these abnormal structures often deviated from the relevant standard range. The microstructure of P92 pipeline is shown in Figure 23. The martensitic lath martensite disappear and a large amount of massive ferrite appear. The hardness of the corresponding part tested is 160HB, far lower than the hardness value of the normal structure state. The metallographic structure of a P91 main steam pipeline is shown in Figure 24. At this location, mechanical performance samples are taken for testing, and the results are shown in Tables 4 and 5. The room temperature mechanical properties and high temperature endurance test results are far below the standard recommended values. The abnormality of the structure is reflected in the performance testing process.

5.3 Comprehensive evaluation method

As mentioned above, to some extent, the microstructure of metallic materials corresponds to their mechanical properties, and aging of the microstructure would inevitably cause changes in mechanical properties. The mechanical properties of martensitic steel with abnormal organization often deviate from the recommended range of standards. Therefore, for the aging evaluation process of 9% Cr martensitic heat-resistant steel, if conditions are met, the comprehensive and accurate evaluation of its mechanical performance indicators should be carried out. For the equipment after operation, a comprehensive evaluation should also be conducted based on factors such as operating time, operating environment, and self-condition.

6. Conclusions

(1) Due to resolution limitations, traditional optical microscopes are not very suitable for observing the microstructure of 9% Cr martensitic heat-resistant steel. The working environment requirements for SEM and TEM are strict, with high requirements for sample preparation, long observation time, and expensive instrument costs, which cannot meet the requirements of on-site real-time and simple observation. LSCM, as a convenient tool with high resolution, is currently highly regarded in the assessment of inspection, observation, and aging.

(2) During the aging process of metallic materials, the microstructure may exhibit morphological dispersion, gradual disappearance of orientation, migration of alloying elements, and re-aggregation and growth of carbides. In the metallographic aging rating process of 9% Cr martensitic heat-resistant steel, the aging that occurs during long-term operation and the abnormal aging of the structure should be distinguished, and the rating process should also be specially explained.

(3) With the increase of operation time, there is inevitably a certain correlation between the changes in the metallographic structure, such as tissue aging, ferrite appearance, disappearance of the martensite phase, and carbide precipitation, and the macroscopic properties of the material. Metallographic observation is only a means of studying material properties and is more suitable for short-term on-site inspections. For the aging evaluation of 9% Cr martensitic heat-resistant steel, or for the safety evaluation of this type of material after operation, it is necessary to combine mechanical performance testing indicators, especially high-temperature and long-term mechanical performance indicators, to make a more accurate comprehensive judgment and provide guidance for the safe operation and use of components.

Funding information

This work was financially supported by the China Datang Corporation Technology Plan Project (Research on heat-resistant materials and welding technology for new ultra supercritical units at temperatures exceeding 630°C).

Author contributions

Cai Wenhe and Zhang Xin: Conceptualization, Methodology. Zhang Kun and Fengyuan Shu: Data curation, Writing – original draft. Zhang Kun and Xin Zhang: Visualization, Investigation. Xin Zhang: Supervision. Wang

Zhichun, Xin Chen and Shi Yang: Writing – review & editing. Jianwei Wang and Li Weili: Methodology, Data curation.

Conflict of interest statement

The authors declare that they have no known competing financial interests or personal relationships that could have appeared to influence the work reported in this paper.

References

[1] Saini, N., Mulik, R.S., Mahapatra, M.M., Study on the effect of ageing on laves phase evolution and their effect on mechanical properties of P92 steel, Mater. Sci. Eng. A, 2018, 716: 179–188

[2] Khayatzadeh, S., Tanner, D.W.J., Truman, C.E., Flewitt, P.E.J., Smith, D.J., Influence of thermal ageing on the creep behaviour of a P92 martensitic steel, Mater. Sci. Eng. A, 2017, 708: 544–555

[3] Zhao, L., Jing, H., Xu, L., An, J., Xia, G., Numerical investigation of factors affecting creep damage accumulation in ASME P92 steel welded joint, Mater. Des., 2012, 34: 566–575

[4] Zhao, D., Li, S., Wang, X., Wang, Y., Liu, F., Cao, X., Proton irradiation induced defects in T92 steels: An investigation by TEM and positron annihilation spectroscopy, Nucl. Instrum. Methods Phys. Res. B, 2019, 442: 59–66

[5] Dak, G., Singh, V., Kumar, A., Sirohi, S., Bhattacharyya, A., Pandey, C., et al., Microstructure and mechanical behaviour study of the dissimilar weldment of 'IN82 buttered' P92 steel and AISI 304L steel for ultra super critical power plants, Mater. Today Commun., 2023, 37: 107552

[6] Hald, J., Microstructure and long-term creep properties of 9-12% Cr steels, Int. J. Press. Vessel. Pip., 2008, 85(1/2): 30–37

[7] Hald, J., Korcakova, L., Precipitate stability in creep resistant ferritic steels- experimental investigations and modeling, ISIJ Int., 2003, 43(3): 420–427

[8] Suzuki, K., Kumai, S., Toda, Y., Kushima, H., Kimura, K., Two-phase separation of primary MX carbonitride during tempering in creep resistant 9Cr1MoVNb steel, ISIJ Int., 2004, 43(7): 1089–1094

[9] Dvorak, J., Kral, P., Sklenicka, V., Kvapilova, M., Sifner, J., Koula, V., et al., Study of creep damage in P92 steel using acoustic emission, Procedia Struct. Integr., 2024, 52: 259–266

[10] Shang, C.G., Wang, M.L., Zhou, Z.C., Yagi, K., Lu, Y.H., The microstructure evolution and its effect on creep behaviors in P92 steel under different stresses, Mater. Charact., 2023, 198: 112744

[11] Lou, M., Niu, S., Ma, Y., Shan, H., Yang, B., Li, Y., The aging characteristics of resistance rivet welded aluminum/steel joints, J. Mater. Res. Technol., 2023, 26: 3615–3628

[12] He, H., Shen, Y., Guo, Y., Precipitates change of P92 steel under 3.5 MeV Fe^{13+} ion irradiation at 400°C, Mater. Charact., 2023, 205: 113273

[13] Dudova, N., Mishnev, R., Kaibyshev, R., Effect of long-term aging on the low cycle fatigue behavior and microstructure of a 10% Cr martensitic steel with low nitrogen and high boron contents at 650°C, Mater. Today Commun., 2024, 38: 108323

[14] Sklenicka, V., Kucharova, K., Svobodova, M., Kral, P., Kvapilova, M., Dvorak, J., The effect of a prior short-term ageing on mechanical and creep properties of P92 steel, Mater. Charact., 2018, 136: 388–397

[15] Maddi, L., Shivhare, R., Kumar, V., Goel, M., Ramesh, M., Ballal, A., Effect of tempering time on the microstructure and stress rupture properties of P92 steel, Mater. Today: Proc., 2021, 44(Part 1): 34–38

[16] Wen, J.-b., Zhou, C.-Y., Li, X., Pan, X.-M., Chang, L., Zhang, G.-D., et al., Effect of temperature range on thermal-mechanical fatigue properties of P92 steel and fatigue life prediction with a new cyclic softening model, Int. J. Fatigue, 2019, 129: 105226

[17] Gao, N., Zhang, W., Yin, P., Liang, F., Zhang, G., Xia, X., et al., Multiaxial fatigue behaviour and damage mechanisms of P92 steel under various strain amplitudes and strain ratios at high temperature, Int. J. Fatigue, 2022, 158: 106774

[18] Junek, M., Svobodová, M., Janovec, J., Horváth, J., Ducháček, P., Long-term thermal degradation of narrow gap orbital welded P91 and P92 steels, Int. J. Press. Vessel. Pip., 2020, 185: 104133

[19] Yang, X., Liao, B., Xiao, F.-r., Yan, W., Shan, Y.-y., Yang, K., Ripening behavior of M23C6 carbides in P92 steel during aging at 800°C, J. Iron Steel Res. Int., 2017, 24(8): 858–864

[20] Xia, X., Zhu, B., Jin, X., Tang, M., Yang, L., Xue, F., et al., Analysis on microstructure and properties evolution and life prediction of P92 steel in high temperature

service, Int. J. Press. Vessel. Pip., 2021, 194(Part A): 104482

[21] Zhang, W., Zhang, T., Wang, X., Chen, H., Gong, J., Remaining creep properties and fracture behaviour of P92 steel welded joint under prior low cycle fatigue loading, J. Mater. Res. Technol., 2020, 9(4): 7887–7899

[22] Dak, G., Sirohi, S., Pandey, C., Study on microstructure and mechanical behavior relationship for laser-welded dissimilar joint of P92 martensitic and 304L austenitic steel, Int. J. Press. Vessel. Pip., 2022, 196: 104629

[23] Xin, Z., Zhigang, Z., Xiaoru, W., Ran, W., Liwei, W., Research progress on reheat cracks in welded joints of power plant boiler pressure pipelines, Mech. Eng. Mater., 2017, 41(2): 8–14 + 111 (in Chinese)

[24] Vaillant, J.C., Vandenberghe, B., Hahn, B., Heuser, H., Jochum, C., T/P23, 24, 911an d 92: new grades for advanced coal fire power plants: properties and experience, Int. J. Press. Vessel. Pip., 2008, 85(1/2): 38–46

[25] Adhithan, B., Pandey, C., Study on effect of grain refinement of P92 steel base plate on mechanical and microstructural features of the welded joint, Int. J. Press. Vessel. Pip., 2021, 192: 104426

[26] Zhang, X., Yanchang, Q., Comparative study of different welding wires on T92 welded joints, Philos. Mag. Lett., 2018, 9(4): 133–138

[27] Meng, L., Research on safety performance of abnormal hardness of P92 steel, Tianjin University, Tianjin, 2013